Benzo annulated cycloheptatriene PCP Pincer Iridium complexes

Wolfgang Leis[a], Sophie Wernitz[a], Benedikt Reichart[b], David Ruckerbauer[b], Johannes Wolfram Wielandt*[b] and Hermann A. Mayer*[a]

Structure comparison

Table S1: Comparison of bond distances in the BCHT complex **9** and the analogous CHT complex[1]

	CHT•Tf in pm	**9**•BF_4 (x-ray) in pm	**9**•BF_4 (opt.) in pm
d(Ir-H)	–	–	159.1
d(Ir-Cl)	249.6	250.8	253.8
d(Ir-CO)	191.6	192.9	192.7
d(Ir-C_{ipso})	209.3	208.2	208.8
d(C-O)	112.7	111.5	115.0
d(Ir-P_1)	234.5	235.2	240.4
d(Ir-P_2)	234.2	234.7	239.3

Table S2: Comparison of bond angles and torsional angles in the BCHT complex **9** and the analogous CHT complex[1]

	CHT•Tf[1]	**9**•BF_4 (x-ray)	**9**•BF_4 (opt.)
	in °	in °	in °
a(Cl-Ir-H)	–	–	175.3
a(Cl-Ir-CO)	95.8	96.2	92.9
a(Cl-Ir-C_{ipso})	83.9	85.1	84.4
a(Cl-Ir-P_1)	100.2	100.6	98.0
a(Cl-Ir-P_2)	92.2	92.8	91.6
a(Ir-C-O)	177.5	175.1	179.8
t(Cl-Ir-C_{ipso}-C_2)	68.7	69.7	67.7
t(H-Ir-C_{ipso}-$C_{2'}$)	–	–	71.2
t(P_1-Ir-C_{ipso}-$C_{2'}$)	-8.6	-6.2	-11.6
t(P_2-Ir-C_{ipso}-C_2)	-24.3	-23.5	-24.6

Table S3: Comparison of the crystal data in the BCHT complex **9** and the analogous CHT complex[1]

	CHT•Tf[1]	**9**•BF_4 (x-ray)	**9**•BF_4 (opt.)
Crystal data	Triclinic, a=911.24(15) pm, b=1486.4(5) pm, c=1561.0(2) pm, α=62.273(18) °, β=87.045(13) °, γ=76.072(16) °, U=1812.02 Å^3, space group P -1.	Monoclinic, a=1309.25(7) pm, b=1235.77(6) pm, c=2336.08(13) pm, α=90.00 °, β=109.700(4) °, γ=90.00 °, U=3558.4(3) Å^3, space group P21/c.	–

Mass spectrometry

Overview of fragments

In the supplementary informations Table S1 collects the mass to charge ratios, the proposed structures, the availability of high resolution mass spectra and the ionisation source of all experimentally verified fragments mentioned so far and in the following.

Table S4 Possible ions in the mass spectra **6**

m/z[a]	structure	source	HR[b]	*m/z*[a]	structure	source	HR[b]
714	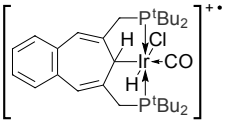	-	-	677	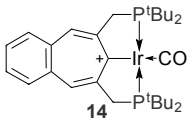 **14**	ESI, FAB	yes
713	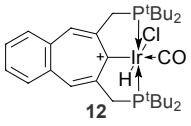 **12**	FAB	no	647	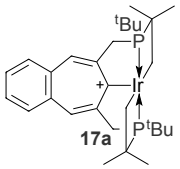 **17a**	ESI, FAB	yes
707	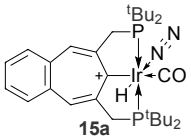 **15a**	ESI	yes	589	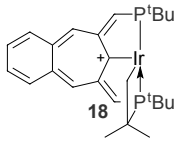 **18**	ESI, FAB	yes
693	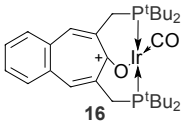 **16**	ESI	yes	531	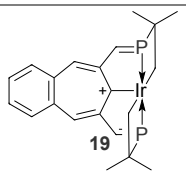 **19**	ESI, FAB	no
685	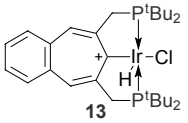 **13**	FAB	no	475	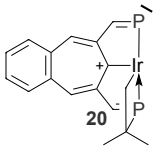 **20**	FAB	no
679	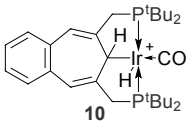 **10**	ESI	yes	419	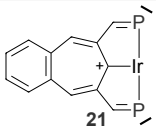 **21**	FAB	no

[a] mono-isotopic mass to charge ratio

[b] high resolution (FTICR) data availability

Routine direct infusion set-up

A 10 µM sample solution was prepared under inert conditions in an HPCL vial with a septum. The inlet of the electro-spray chamber is connected to a transfer tube (PEEK) with or without an in-line filter and the syringe as well as the tubing are flushed with the dry solvent. Subsequently the sample is drawn up with the syringe, connected to the transfer tube and injected at a flow of 1 - 20 µL/min with the syringe pump.

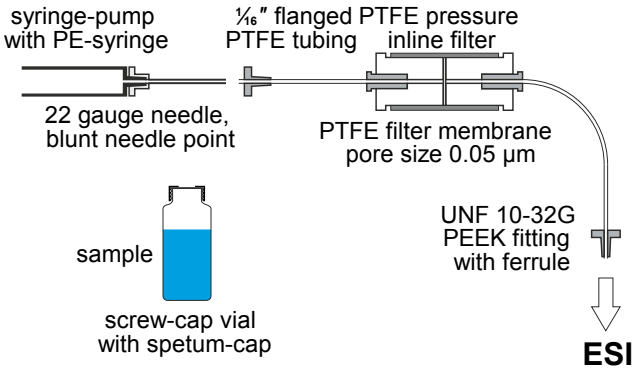

Figure S1: Routine direct infusion set-up

Improved direct infusion set-up

Comparing Figures S1 and S2 it is apparent that the routine set-up is extended by an assembly of 3-way-valves. The central valve is the connection to the argon source and allows the flushing of the syringe and the tubing. An screw-cap vial containing the sample solution is connected to the left-hand side 3-way-valve. The right-hand side valve is linked to a glass bottle, which is equipped with a distributor and for pressure equilibration with the argon source. Prior to injecting the sample, the dried cleaning solvent from the glass bottle is drawn up with the syringe and the complete assembly is flushed three times to remove water from the assembly surfaces. Subsequently, the sample solution is drawn up to the syringe and injected to the electro-spray chamber having all other lines closed.

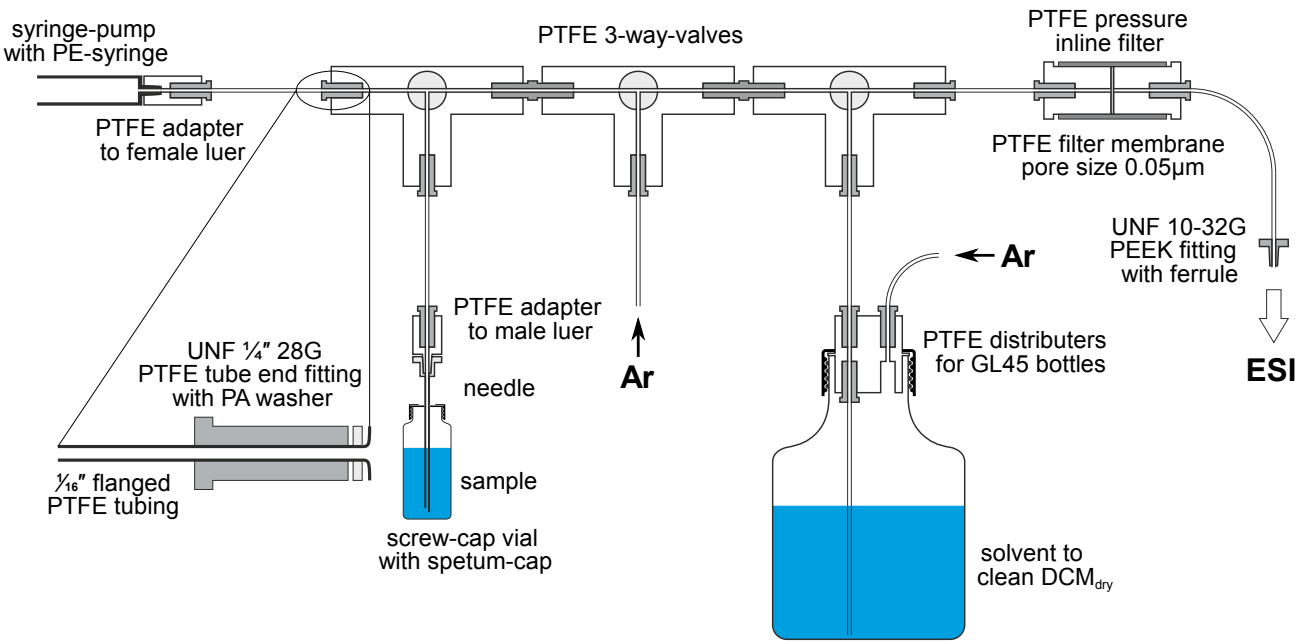

Figure S2: Direct infusion set-up for air / moisture sensitive compounds

All components of the transfer assembly which are in contact with the sample solution are made of PTFE. Either a gas-tight 1 mL glass syringe or a disposable 1 mL PE syringe is connected to the transfer assembly *via* a female luer adapter. A combination of a male luer adapter and a hypodermic needle is used to attach the screw-cap vial to the improved infusion set-up. The not explicitly mentioned connections as the tube to valve transitions are realised with BOLA tube end fittings (UNF ¼″ 28G) and flanges or BOLA double tube end fittings. The complete dead volume of the assembly doubles with approximately 70 µL as compared to the routine infusion set-up with about 20 µL (Figure 6).

Reaction of 6a with $Ph_3C\ BF_4$ and pure oxygen

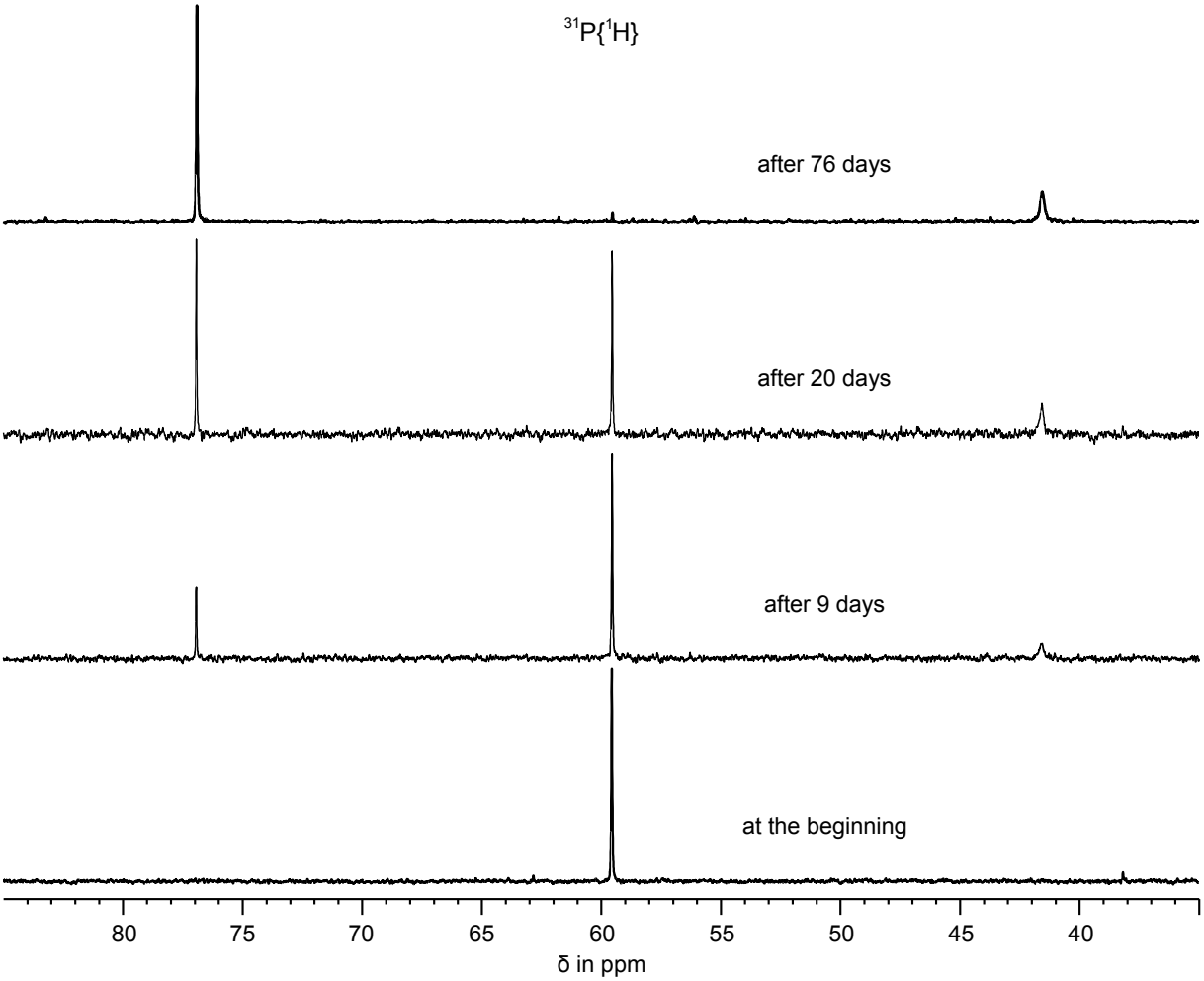

Figure S3: $^{31}P\{^1H\}$ spectra of the reaction solution, containing **6a**, $Ph_3C\ BF_4$ and O_2 over a period of 2.5 months.

Additional theoretical details

Energy differences

For a given reaction equation (1):

$$A + B \rightarrow C + D \quad (1)$$

the energy differences (ΔE), corresponding to the energy of formation (in the gas phase) of the respective reaction, were calculated according to equation (2).

$$\Delta E = (E_{tot}(C) + E_{tot}(D)) - (E_{tot}(A) + E_{tot}(B)) \quad (2)$$

$E_{tot}(X)$ is the total electronic energy of the structure of the compound X, obtained from the final step of the geometry optimisation in Jaguar. For each complex in a figure the energy difference is calculated for a reaction starting from the reference compound [A] and if needed further reactants [B] leading to the respective complex [C] and possibly other products [D]. The reference compound [A] is usually mentioned in the figure caption and defines the zero point of the energy scale in this figure.

Structures

Table S5 Structures obtained from geometry optimisation B3LYP/LACVP* (methyl groups and some hydrogen atoms are omitted for clarity).

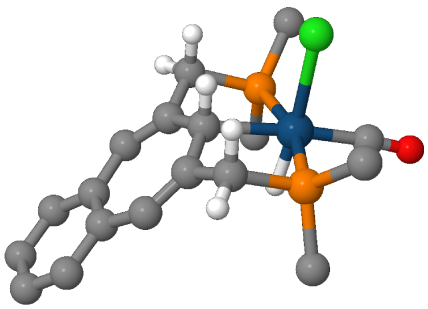 **6a**	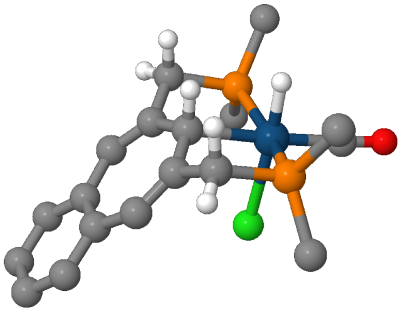 **6b**	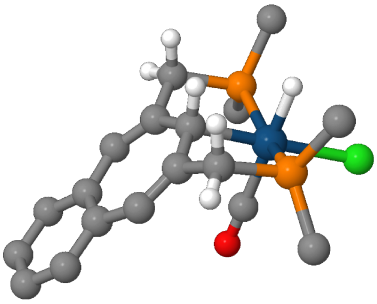 **6c**
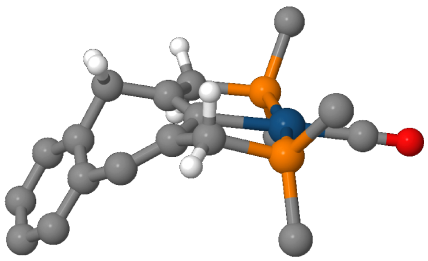 **8a**	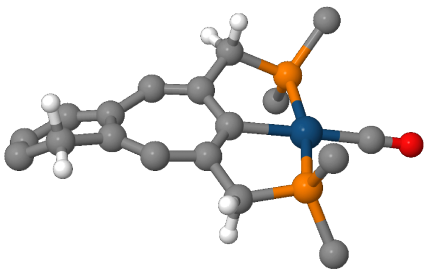 **8b**	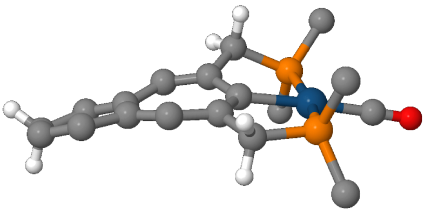 **8c**
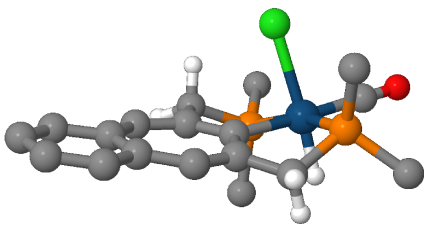 **9**	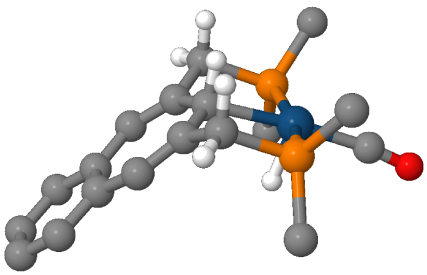 **10**	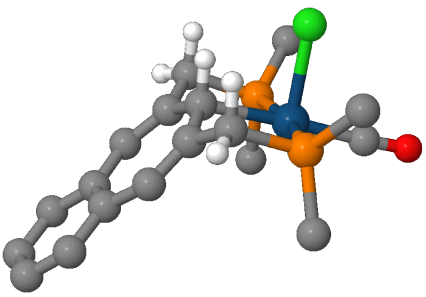 **11**
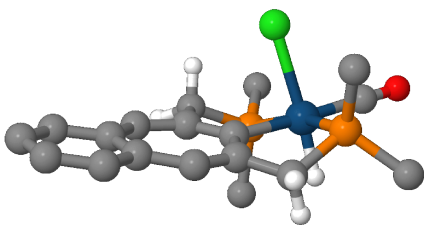 **12**	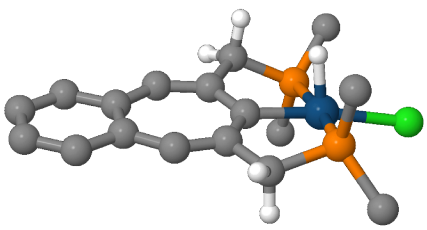 **13**	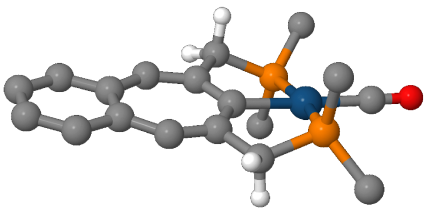 **14**
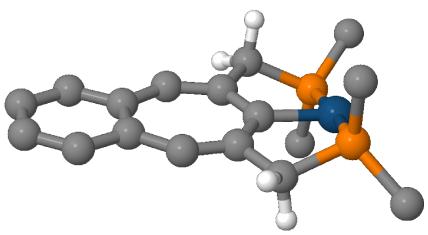 **14'**	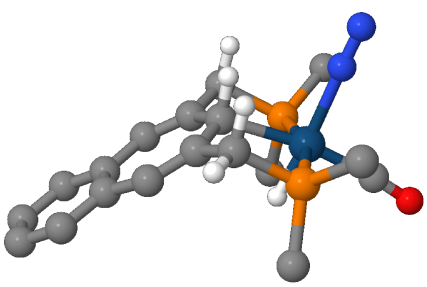 **15a**	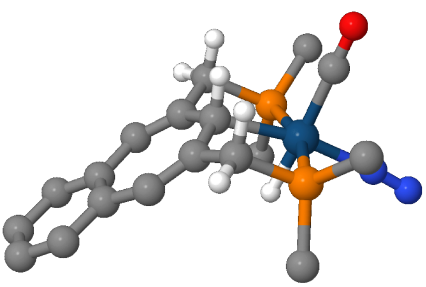 **15b**

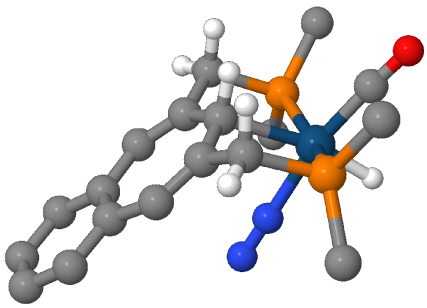

15c

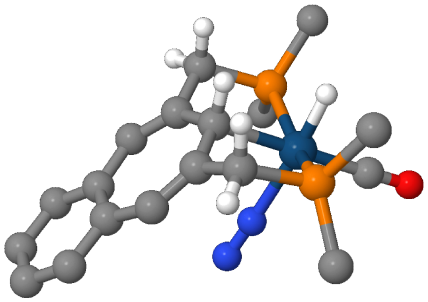

15d

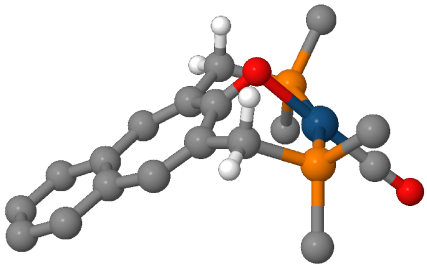

16

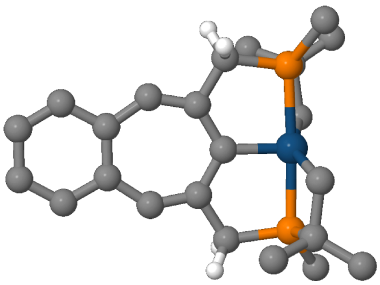

17a

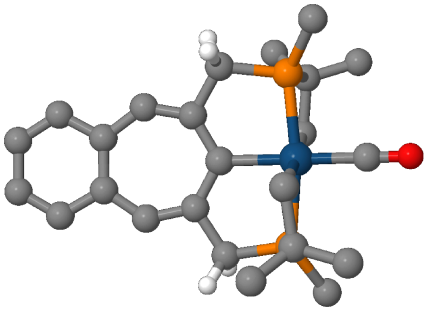

17a'

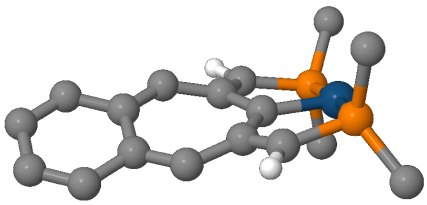

17b

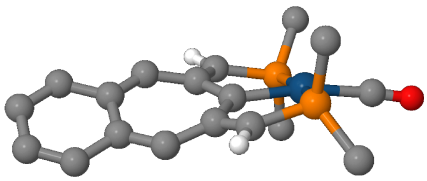

17b'

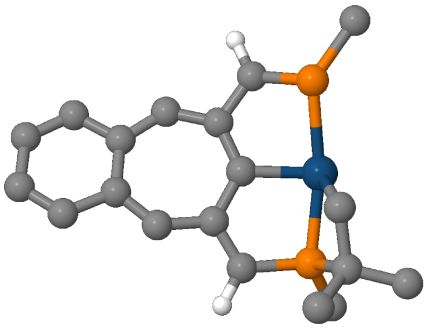

18

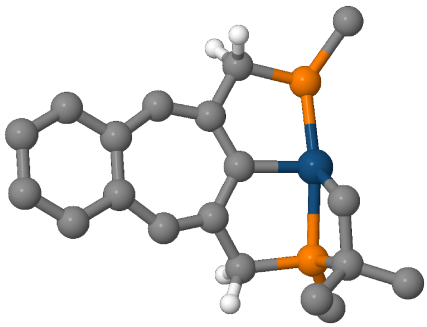

18'

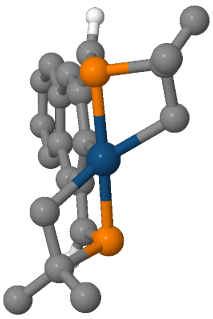

19

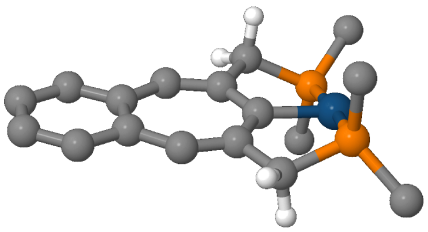

19'

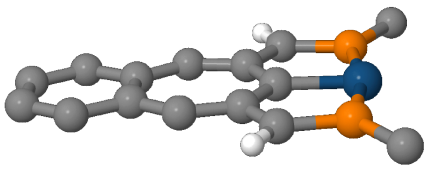

19''

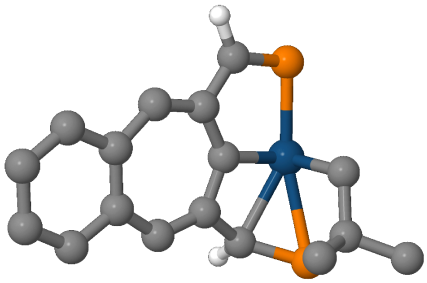

20

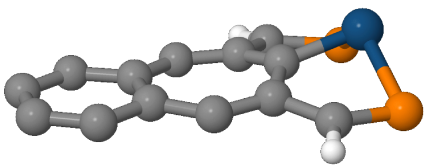

21

DFT results of some peroxide and oxo species

Table S6 Structures (according to Figure S4 and missing in Table S5) obtained from geometry optimisation B3LYP/LACVP* (methyl groups and some hydrogen atoms are omitted for clarity).

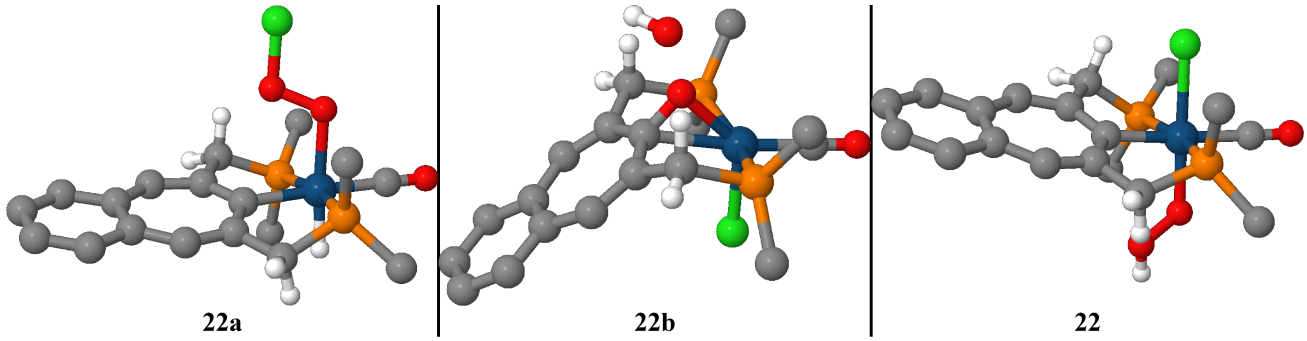

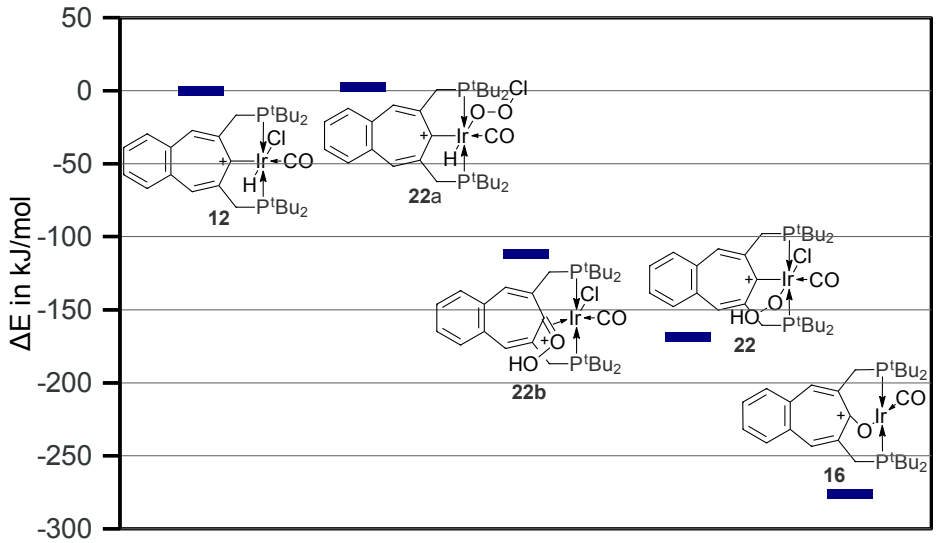

Figure S4: DFT energies (relative to the energy of **12**) of some possible intermediates on a reaction coordinate leading to the oxo complex **16**.

Additional experimental details

Alternative approaches for bromination yielding BCHT dibromide (3)

Bromination with CBr_4/PPh_3:

To a cooled solution (0 °C) of **2** (1.00 g, 4.94 mmol) and tetrabromomethane (3.44 g, 10.38 mmol) in DCM (8 ml) a solution of triphenylphosphine (3.27 g, 12.46 mmol) in DCM (4 ml) was added drop wise over a period of 20 min. The mixture was allowed to warm to room temperature and stirred for 14 h. The reaction was quenched through addition of silicagel. After evaporation of the solvent, the orange residue was eluted over silicagel with a mixture of ethyl acetate and petroleum ether (1:4, 150 ml). Evaporation of the solvent yielded a brown liquid. The crude product was purified by column chromatography yielding an off-white solid (SiO_2, cyclohexane:DCM = 3:1). Yield: 24 %.

Bromination with HBr/acetic acid:

2 (350 mg, 1.73 mmol) was dissolved in hydrobromic acetic acid solution (8 ml) and heated to 95 °C for 10 h. The reaction was quenched through addition of water. The solids were removed via filtration and the volatile parts of the filtrate were removed under vacuum. The orange residue was dissolved in ethyl acetate and extracted with water. The combined organic layers were dried over Na_2SO_4 and evaporated to dryness. The crude product was purified by column chromatography yielding an off-white solid (SiO_2, cyclohexane:DCM = 3:1). Yield: 15 %.

Bromination with tetrabutylammonium bromide/ boron trifluoride diethyl etherate:

A mixture of **2** (0.61 g, 3.00 mmol) and tetrabutylammonium bromide (2.90 g, 9.00 mmol) were suspended in DCM (15 ml). Boron trifluoride diethyl etherate (1.28 g, 9.00 mmole) was added over a period of 10

min. The suspension was heated to 40°C for 5 h. The reaction was quenched through addition of saturated $NaHCO_3$ solution. The aqueous layer was extracted with DCM (50 ml). The combined organic layers were extracted with Brine, dried over Na_2SO_4 and evaporated to dryness. The crude product was purified by column chromatography yielding an off-white solid (SiO_2, cyclohexane:DCM = 3:1). Yield: 68 %.

References

1. A. M. Winter, K. Eichele, H.-G. Mack, W. C. Kaska, and H. A. Mayer, *Organometallics*, 2005, **24**, 1837–1844.